buildings

MDPI

Article

Study on Early Age Concrete's Compressive Strengths in Unmanaged Curing Condition Using IoT-Based Maturity Monitoring

Sanghee Kim [1], Donghyuk Jung [2,*], Ju-Yong Kim [1] and Ju-Hyun Mun [1]

[1] Department of Architectural Engineering, Kyonggi University, Suwon 16227, Republic of Korea; sanghee0714@kyonggi.ac.kr (S.K.); ju2020@kyonggi.ac.kr (J.-Y.K.); mjh@kgu.ac.kr (J.-H.M.)
[2] School of Civil, Environmental and Architectural Engineering, Korea University, Seoul 02841, Republic of Korea
* Correspondence: jungd@korea.ac.kr

Abstract: Although accurately estimating the early age compressive strength of concrete is essential for the timely removal of formwork and the advancement of construction processes, it is challenging to estimate it in cool, cold, hot, or unmanaged conditions. Various nondestructive testing methods, including recent IoT-based techniques, have been proposed to determine the compressive strength of concrete. This study evaluates the maturity method using the wireless thermocouple sensor in assessing the early age compressive strength of concrete slabs, particularly those not subjected to watering and protection in a cool environment below 20 °C. For this purpose, wire and wireless thermocouple sensors were installed in reinforced concrete (RC) slabs, whereas wire thermocouple sensors were installed in concrete cylinders. In addition, the compressive strengths of standard-cured cylinders, field-cured cylinders, and core samples extracted from the RC slab were measured. On day 7, the maturity index (M) values for the field-cured cylinders were 7% lower than those of the standard-cured cylinders, and the M values for the RC slabs with wire and wireless sensors were 6% lower. The compressive strengths of the field-cured cylinders and core samples extracted from the RC slabs were 19% and 14% lower than those of the standard-cured cylinders, respectively. Thus, while the difference in M values was 6–7%, the difference in compressive strength was significantly higher, at 14–19%. In a cool environment without watering or protection, the difference in strength can be even greater. Consequently, a commercial IoT-based thermocouple sensor can replace conventional wire sensors and adopt to estimate early age compressive strength of concrete in unmanaged curing condition.

Keywords: wireless thermocouple sensor; nondestructive testing (NDT); maturity method; concrete; early age compressive strength; unmanaged curing conditions; cool environment

Citation: Kim, S.; Jung, D.; Kim, J.-Y.; Mun, J.-H. Study on Early Age Concrete's Compressive Strengths in Unmanaged Curing Condition Using IoT-Based Maturity Monitoring. *Buildings* **2024**, *14*, 798. https://doi.org/10.3390/buildings14030798

Academic Editor: Grzegorz Ludwik Golewski

Received: 2 February 2024
Revised: 4 March 2024
Accepted: 12 March 2024
Published: 15 March 2024

1. Introduction

In reinforced concrete (RC) structures, compressive strength of concrete is a critical indicator for assessing structural safety. RC structures are generally designed by considering their 28-day curing strength. Because the compressive strength of fresh concrete develops through hydration, delaying subsequent construction processes until after 28 days of curing can pose significant challenges in building construction. The removal of formwork is a key process during the subsequent process, and the need for smart formwork to enhance efficiency, safety, and sustainability is raised to overcome the shortcomings of conventional formwork [1]. Construction processes often proceed once the minimum compressive strength sufficient for the subsequent stages is secured. Consequently, accurately predicting early age compressive strength is critical for the progression of construction processes [2–4]. The concrete matrix is a composite of various components, making it very difficult to accurately predict and measure the early age compressive strength [5,6]. Therefore, various direct and indirect methods have been developed to determine the compressive strength of concrete structures [4,7–9]. Direct methods include core extraction from concrete structures for compressive strength measurements [10,11]. Indirect methods, established by the American Society for Testing and Materials (ASTM), encompass the rebound method [12], penetration resistance method [13], pull-out test [14], pull-off test [15], ultrasonic pulse velocity [16], maturity method [17], and cast-in-place cylinders [18], each with standardized procedures. ACI 228.1R-19 [8] reviewed the nondestructive measurement methods provided by the ASTM, reporting on the analysis of results and acceptance criteria.

According to the Korean Construction Standard KCS 14 20 10 [19], the formwork panels of foundations, sides of beams, columns, and walls can be removed when the compressive strength of cylinders cured under the most adverse conditions on site reaches 5 MPa or more. Alternatively, in temperatures ranging from 10 °C to below 20 °C, these formwork panels can be dismantled after 6 days without evaluating their compressive strength if ordinary Portland cement concrete is used. However, the formwork under the slabs, beams, and inner surface of the arches in a single-layer structure can be removed only when the design's compressive strength reaches at least 2/3 or a minimum of 14 MPa. In a multilayer structure, this is only permissible when the strength exceeds the design's compressive strength.

The maturity method is a nondestructive technique for predicting concrete strength by utilizing the heat generated from chemical reactions between water and cement based on the relationship between thermal history and concrete strength development. Various studies have been conducted on the development of the concrete compressive strength based on maturity [10,20–22]. Embedding a wire thermocouple sensor in concrete is an essential step of the maturity method, and a data logger is installed to receive and record temperature data from the thermocouple. This poses difficulties in measuring the hydration heat at multiple points and requires the equipment to be stationed for long durations. Recent equipment advancements have led to the development of wireless thermocouple sensors, prompting research on their applicability [23–26]. Of course, the price of the wireless sensor is approximately four times higher than that of a wire sensor, but the installation and operation costs of the datalogger are saved, and it can be installed in multiple places simultaneously. Kampli et al. [23] investigated the concrete strength development using a system capable of transmitting hydration heat data in real time to a data cloud through a WiFi-enabled wireless temperature sensor. Miller et al. [24] developed an IoT-enabled monitoring system and assessed its usability. Mun et al. [25] conducted a comparative study between a wireless relative humidity and temperature (RH&T) sensor and a thermocouple to assess the applicability of the RH&T in cumulative temperature methods, and Lee et al. [26] evaluated the compressive strength in winter conditions using the wireless sensor SmartRock2, considering the use of an insulated formwork.

There are research papers related to the development of concrete strength in cold or hot curing conditions, but few studies have simultaneously focused on unmanaged and cool curing conditions. Therefore, in line with recent research trends and the need for data on the development of concrete strength in harsh curing conditions, this study aims to evaluate the feasibility of IoT-based wireless thermocouple sensors in assessing the early age compressive strength of RC slabs under unprotected and unwatered conditions in an environment below 20 °C. For this purpose, wire sensors and wireless Bluetooth sensors were used to measure the temperature–time history of the RC slabs and field-cured concrete cylinders. Additionally, to elucidate the relationship between the maturity and development of concrete, the compressive strengths of standard-cured cylinders, field-cured concrete cylinders, and core samples extracted from the RC slabs were evaluated. Through the experimental results, this study aimed to confirm the feasibility of IoT-based wireless thermocouple sensors for assessing the early age compressive strength of RC slabs under specific curing conditions.

2. Test Program

2.1. Test Specimens

Experiments were conducted to measure the hydration heat using wire/wireless thermocouple devices under cool weather conditions and to evaluate the compressive strength of early age concrete based on these measurements (Table 1). These experiments can be divided into two main categories. The first compares the hydration heat (wire/wireless sensor) of an RC slab with that of standard- or field-cured specimens (wire sensor), and the second compares the compressive strength of core samples from the RC slab as well as standard- and field-cured cylinders. For this purpose, two RC slabs were fabricated for core extraction and hydration heat measurements, along with standard- and field-cured cylinders.

Table 1. Test plan.

<table>
<tr><th colspan="2" rowspan="2">Curing Type and Sensor</th><th colspan="6">Days</th></tr>
<tr><th>1</th><th>3</th><th>7</th><th>14</th><th>28</th><th>91</th></tr>
<tr><td>Standard curing</td><td>Cylinder</td><td rowspan="2">5 * samples</td><td>5 samples</td><td>5 samples</td><td>5 samples</td><td>5 samples</td><td>5 samples</td></tr>
<tr><td rowspan="2">Field curing</td><td>Cylinder</td><td>5 samples</td><td>5 samples</td><td>5 samples</td><td>5 samples</td><td>5 samples</td></tr>
<tr><td>Wire sensor</td><td colspan="3">5 samples measured</td><td></td><td></td><td></td></tr>
<tr><td rowspan="3">Reinforced concrete slab</td><td>Core sample</td><td>-</td><td>-</td><td>5 samples</td><td>5 samples</td><td>5 samples</td><td>5 samples</td></tr>
<tr><td>Wire sensor</td><td colspan="3">5 points were measured</td><td colspan="3">Not available</td></tr>
<tr><td>Wireless sensor</td><td colspan="3">5 points were measured</td><td colspan="3">Not available</td></tr>
</table>

* The cylinders used for compressive strength testing in 24 h were the same.

Standard curing: The first experimental group consisted of standard-cured cylinders, with 30 specimens of Ø100 × 200 mm manufactured according to ASTM C31/C31M [27]. These specimens were also constructed alongside the RC slab and initially cured for 24 h next to the RC slab. After this period, the five cylinders were demolded, and their compressive strengths were evaluated according to ASTM C31/C31M [27]. The rest, totaling 25 demolded cylinders, were kept in a water tank, maintaining a temperature of 20 °C. The compressive strengths of the five specimens were evaluated on days 3, 7, 14, 28, and 91 post-pouring.

Field curing: The second experimental group involved field-cured cylinders, with 30 specimens of Ø100 × 200 mm manufactured according to ASTM C31/C31M [27] and cured alongside the RC slabs. Of these, five had wire sensors embedded, which recorded the temperature–time history (Figure 1b), and all the cylinders were cured under the same conditions as the RC slabs. The compressive strengths of the five specimens were evaluated on days 3, 7, 14, 28, and 91 post-pouring. However, as the field-cured and standard-cured cylinders were cured under identical conditions for the first 24 h after pouring, additional specimens were not required to measure the 1-day compressive strength of the field-cured cylinders.

RC slab: The third group of specimens consisted of two RC slabs as structural elements. The hydration heat was measured from the RC slab using wire and wireless thermocouple sensors, and the compressive strengths of the extracted core samples were evaluated. Two RC slabs measuring 980 × 2500 × 200 mm^3 (width × length × thickness) were constructed as structural elements (Figure 2). To prevent temperature cracking in the slabs, SD400 D10 reinforcement bars were placed at intervals of 260–360 mm. The locations of the bars were strategically planned to mitigate the influence of reinforcement bars on core extraction. To measure the concrete compressive strength by core extraction, five cores were taken on days 5, 12, and 26 after drying for 2 d, and their compressive strengths were measured on days 7, 14, and 28. Cores were extracted using a drill with a Ø100 mm nominal diameter, which had an actual inner diameter of 99.5 mm. During the experiment, to simulate harsh curing conditions, the concrete structure slabs were cured without any protection using a nonwoven fabric or watering after pouring. Furthermore, to replicate the actual RC slab environment, supports were placed underneath the slab to create space. Both the wire and wireless thermocouple sensors were embedded into one RC slab as planned (Figures 1a and 2). For the IoT-based wireless thermocouple product, the commercially available SmartRock was used. The specification of SmartRock's reading range is −30~+85 °C, measurement accuracy ± 1 °C, measurement frequency of 15 min, and battery life of up to 4 months. Core samples were extracted from the RC slabs, as shown in Figure 2b, by intentionally avoiding the steel bars.

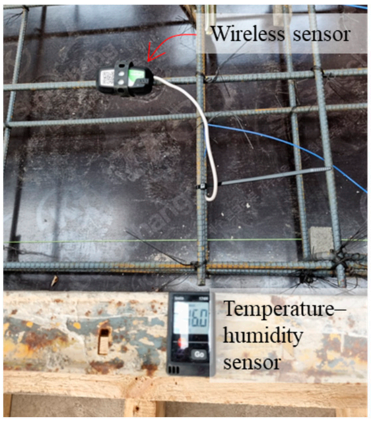

Installation of wireless sensor and temperature–humidity sensor

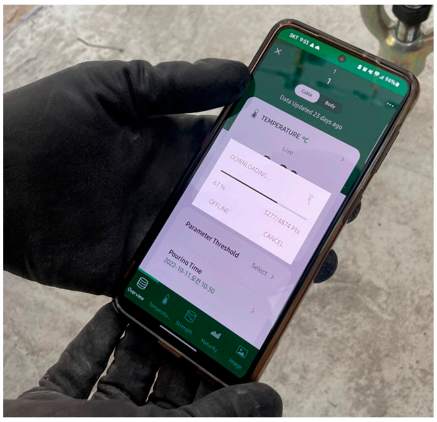

Acquirement of data

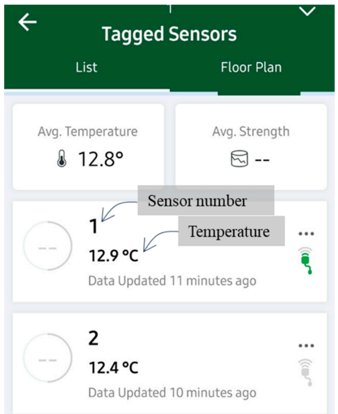

Received data

(**a**) Wireless thermocouple sensors in RC slab

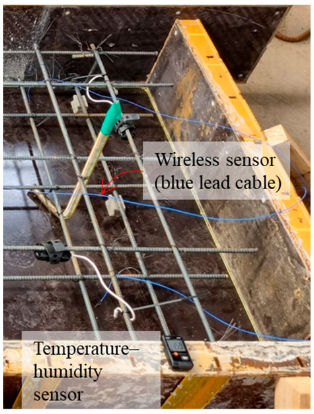

Wire sensor

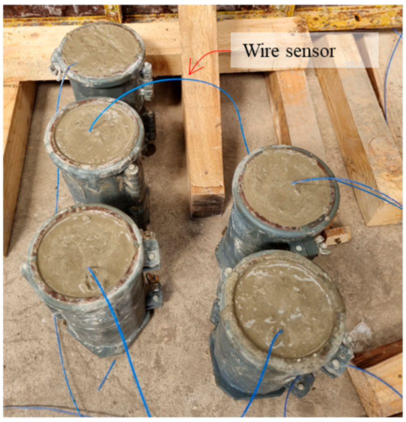

Wire Sensor in field-cured cylinder

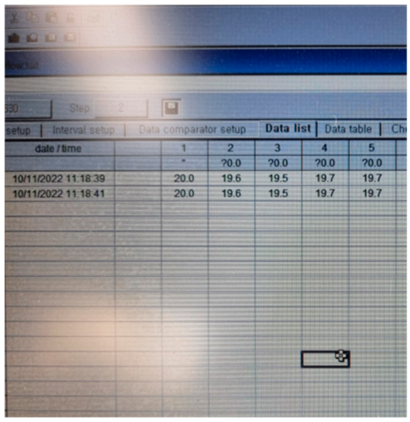

Acquirement of data from the wire sensor

(**b**) Wire thermocouple sensor in RC slab and cylinder

Figure 1. Installation of thermocouple and acquirement of data.

Curing condition: Considering the unfavorable concrete curing conditions, the experiment was scheduled for October 2022, known for its cool weather, and any watering and protection efforts were forgone. For reference, the weather in South Korea during October is cool, with an average temperature of 16.7 °C and an average humidity of 71.7% over the past three years (2019–2021).

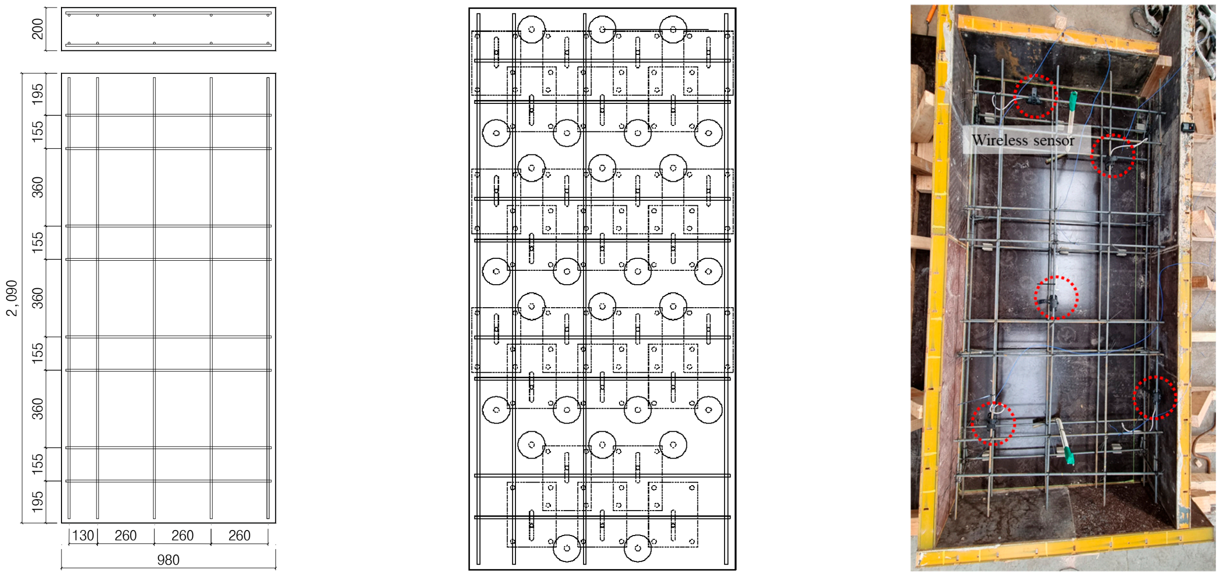

(**a**) RC slab (**b**) Core sample extraction (**c**) Location of wire/wireless sensors

Figure 2. Reinforced concrete (RC) slab dimensions, core plan, and wireless sensor location (units in mm).

2.2. Materials

The concrete used for the experiment was ready-mix concrete with a 28-day nominal strength of 24 MPa and a slump of 150 mm (Table 2). The maximum size of the coarse aggregate was 25 mm, the slump was 150 mm, and the air content was 4.5 ± 1.5%. The mixing water had a pH of 7.0, and the reclaimed water usage ratio was 30%.

Table 2. Mix proportion (weight ratio).

Mix.	W/B	S/a	Binder	Water	Aggregate		Admixture	AE Agent
Code.	(%)	(%)	(kg/m^3)	(kg/m^3)	Fine (kg/m^3)	Coarse (kg/m^3)	(kg/m^3)	(kg/m^3)
25-24-150	46.6	51.7	335	119	881	831	29	2.55 (1.62%)

The cement used in the ready-mix concrete was blast furnace slag cement Type 2 according to KS L 5210 [28], with a slag content exceeding 30% but less than 60%, Blaine-specific surface area of over 3000 cm^2/g, loss on ignition (LOI) of less than 3.0%, and chloride content of less than 0.3 kg/m^3.

Natural sand was used as the fine aggregate with a bulk density, fineness modulus, and chloride content of 2.57 g/cm^3, 2.85, and 0.4%, respectively. Crushed concrete aggregate was used as the coarse aggregate, with a bulk density and fineness modulus of 2.60 g/cm^3 and 6.85, respectively (Table 3).

Table 3. Properties of aggregate.

Aggregate	**Maximum Size (mm)**	**F.M (Fineness Modulus)**	**Density (g/cm^3)**	**Water Absorption (%)**
Fine	5	2.85	2.57	1.2
Coarse	25	6.85	2.6	0.4

The admixture used was Type 2 fly ash according to KS L 5405 [29], with a density of 2.22 g/cm^3, LOI of less than 5.0%, and Blaine-specific surface area of over 3000 cm^2/g.

3. Test Results

3.1. Ambient Temperature and Humidity

Concrete pouring began at approximately 10 a.m. on 11 October 2022. From 11 a.m., when the construction of the RC slabs and cylinders was complete, the air temperature and humidity at the RC slab and cylinder storage locations were recorded. Measurements were performed at two points every 15 min, and the average values are shown in Figure 3. The first 24 h post-pouring had an average temperature of 15 °C and humidity of 71%, followed by 16.4 °C and 70.2% after 3 days, and 17 °C and 69% after 7 days.

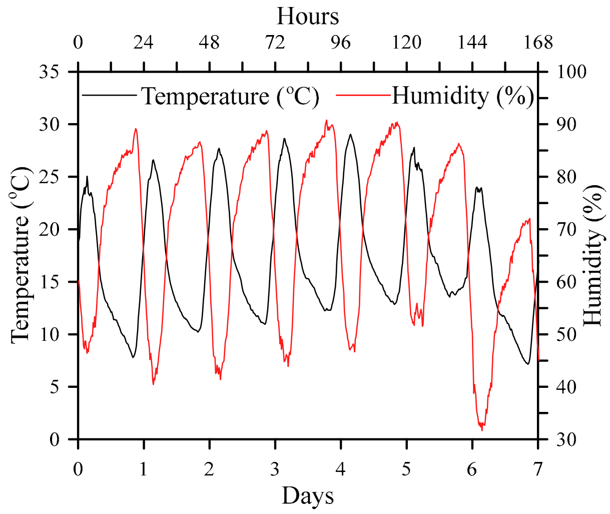

Figure 3. Histories of temperature and humidity in 7 days (=168 h).

3.2. Maturity

To examine the relationship between the early age compressive strength and hydration heat of the RC slab's concrete, five wire thermocouple sensors and five wireless thermocouple sensors were installed in the RC slab. Additionally, wire thermocouple sensors were installed in five field-cured cylinders, and the data obtained was classified as "Wire-slab", "Wireless-slab", and "Wire-field". For the standard-cured cylinders, the hydration heat up to 24 h was assumed to be the same as that measured by the wire field. From 24 to 168 h, it was assumed that the temperature of the water tank containing the cylinders equaled the hydration heat of the concrete specimens. This data was classified as "Standard". The hydration heat was measured for 7 days (168 h) from the time of pouring. The maturity index (M) (Equation (1)) was calculated using the Nurse–Saul maturity [30]:

$$M = \sum_{0}^{t} (T - T_0)\Delta T \qquad (1)$$

where M is the maturity index (°C·h), T is the average temperature of concrete in ΔT, ΔT is the time interval, and T_0 is the datum temperature, which was set to -10 °C in this study [21].

The maturity indexes for wire slab, wireless slab, wire field, and standard were accumulated at 1-h intervals on day 1 and at 6-h intervals on days 3 and 7, as shown in Table 4 and Figure 4. The maturity index for standard curing during the initial 24 h corresponds to the maturity index of the wire field.

Table 4. Results of maturity.

Day	Hour	Maturity Index (°C·h)			
		Wire Slab	Wireless Slab	Wire Field	Standard
1	0	0	0	0	0
	1	31	30	30	30
	2	61	61	61	61
	3	92	92	91	91
	4	124	123	122	122
	5	155	154	153	153
	6	187	185	184	184
	7	218	216	215	215
	8	250	248	246	246
	9	281	278	277	277
	10	312	309	308	308
	11	343	339	338	338
	12	374	370	369	369
	13	405	400	399	399
	14	436	431	430	430
	15	467	461	460	460
	16	497	491	490	490
	17	527	520	519	519
	18	557	549	548	548
	19	585	577	576	576
	20	614	605	604	604
	21	641	632	631	631
	22	668	658	657	657
	23	695	685	684	684
	24	723	712	711	711
2	30	900	886	886	891
	36	1080	1066	1063	1071
	42	1246	1249	1226	1251
	48	1401	1431	1379	1431
3	54	1573	1606	1550	1611
	60	1751	1777	1725	1791
	66	1917	1942	1888	1971
	72	2073	2103	2041	2151
4	78	2248	2259	2213	2331
	84	2427	2411	2389	2511
	90	2594	2564	2554	2691
	96	2753	2723	2710	2871

Table 4. *Cont.*

Day	Hour	Maturity Index (°C·h)			
		Wire Slab	Wireless Slab	Wire Field	Standard
5	102	2930	2893	2884	3051
	108	3111	3069	3063	3231
	114	3282	3250	3230	3411
	120	3444	3429	3389	3591
6	126	3624	3603	3567	3771
	132	3802	3773	3743	3951
	138	3970	3939	3907	4131
	144	4130	4099	4066	4311
7	150	4297	4256	4231	4491
	156	4458	4409	4388	4671
	162	4605	4562	4532	4851
	168	4741	4723	4665	5031

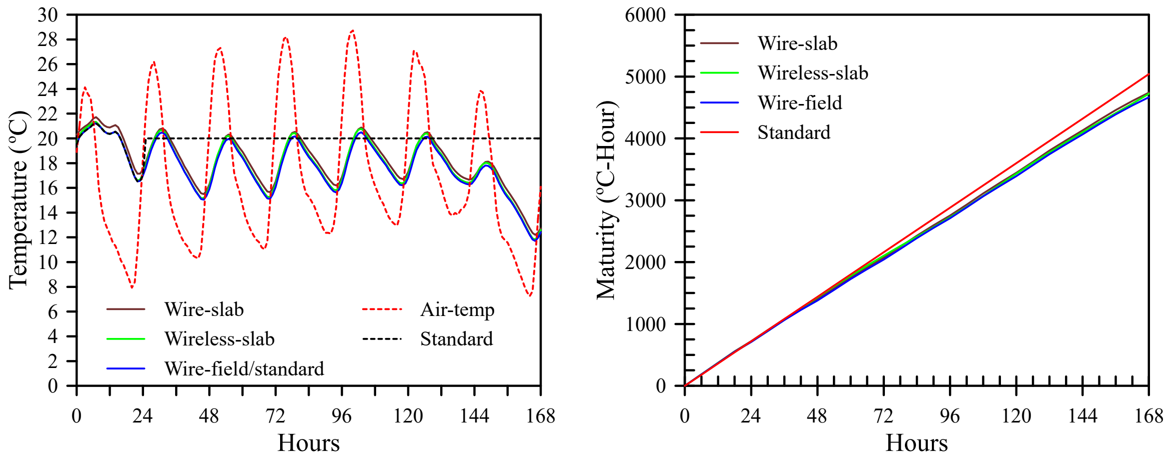

(**a**) Temperature (**b**) Maturity

Figure 4. Comparison of maturity according to curing and/or measurement type in 7 days (168 h).

According to the results, the maturity index (*M*) values for wire slab, wireless slab, wire field, and standard at day 1 (24 h) were 723 °C·h, 712 °C·h, 711 °C·h, and 711 °C·h, respectively (Table 4 and Figure 4). The *M* values for wire slab and wireless slab were 12 °C·h and 1 °C·h higher than those for wire field/standard, respectively. The hydration heat for wire slab was consistently the highest throughout the 24-h period, aligning with the commonly observed trend of elevated hydration heat in structures. Given the increase in concrete temperature at approximately 14 h post-pouring, it is inferred that significant hydration activity occurred at this time.

At day 3 (72 h), the *M* values for wire slab, wireless slab, wire field, and standard were 2073 °C·h, 2103 °C·h, 2041 °C·h, and 2151 °C·h, respectively (Table 4 and Figure 4). Since standard-cured concrete cylinders were kept in a 20 °C water tank after 24 h, they had relatively higher *M* values. The *M* values for wire slab, wireless slab, and wire field were 78 °C·h, 48 °C·h, and 110 °C·h lower than standard, respectively.

At day 7 (168 h), the *M* values for wire slab, wireless slab, wire field, and standard were 4741 °C·h, 4723 °C·h, 4665 °C·h, and 50,311 °C·h, respectively (Table 4 and Figure 4).

The M values for wire slab, wireless slab, and wire field were 290 °C·h, 308 °C·h, and 966 °C·h lower than standard, respectively.

Figure 4a indicates that the peak temperatures for wire slab, wireless slab, and wire field were slightly over 20 °C until day 6 but dropped to approximately 17 °C on day 7. On the seventh day, the temperature variation, with a range of approximately 8 °C, was notably higher than on the preceding days. This significant temperature fluctuation is likely attributable to a marked decrease in ambient temperature on day 7.

3.3. Compressive Strength Development

The compressive strength was measured for five specimens each of the standard-cured cylinders, field-cured cylinders, and core samples extracted from the RC slab on days 1, 3, 7, 14, 28, and 91.

Microcracks can occur in the concrete matrix due to high-speed drilling during core extraction, potentially reducing the compressive strength of the core samples. Additionally, the influence of reinforcement bars on core extraction from RC structures was studied. Jo et al. [31] conducted experiments considering variables such as core area, water–binder ratio, and concrete age, finding that Ø100 × 200 mm cores showed an 11% reduction in strength, while Ø150 × 300 mm cores showed a 4% reduction. Similarly, Oh et al. [32] manufactured Ø100 × 200 mm core specimens from 600 × 600 × 200 mm^3 square test specimens and compared their compressive strength with standard specimens, noting a difference of 11.3%. Based on previous studies, the core extraction locations were carefully chosen to mitigate the influence of reinforcement bars in this study. To account for the damage caused by the core extraction when measuring the compressive strength of the core samples, the formula (Equations (2) and (3)) provided by ACI 214.4R-03 [11] was applied to calculate the equivalent in-place strength. ACI 214.4R does not consider the influence of the reinforcement bars in correcting the compressive strength of the core cylinders.

$$f_{c-eq} = F_{l/d} F_{dia} F_{mc} F_d f_{core} \tag{2}$$

$$F_{l/d} = 1 - \left(0.144 - \alpha f_{core} (2 - l/d)^2\right) \tag{3}$$

where $f_{c\text{-}eq}$ is the equivalent in-place strength, $F_{l/d}$ is the correction factor related to the length-to-diameter ratio, F_{dia} is the correction factor related to the diameter, F_{mc} is the correction factor related to the moisture condition of the core, F_d is the damage factor due to drilling, and f_{core} is the core strength. Because the diameter of the core samples was 99.5 mm, F_{dia} was set to 1.0, F_{mc} to 0.96 (after 48 h of drying), and F_d to 1.06 considering the damage caused by drilling. Here, α is $4.3(10^{-4})1/\text{MPa}$.

The measured compressive strengths (f_c) of the standard-cured cylinders, field-cured cylinders, and the equivalent in-place strengths of the core samples ($f_{c\text{-}eq}$) are summarized in Table 5. The ACI reports that damage during core extraction can lead to a 1.8% reduction in strength.

Table 5. Measured compressive strengths *.

Days	Field-Cured Cylinders					Standard-Cured Cylinders					Core Samples				
	No.	L (mm)	Peak Load (kN)	f_c (MPa)	SD	No.	L (mm)	Peak Load (kN)	f_c (MPa)	SD	No.	L (mm)	Peak Load (kN)	$f_{c\text{-}eq}$ (MPa)	SD
1 d	A1-1	193.5	5.3	0.7	−0.1	A1-1	193.5	5.3	0.7	−0.1	None				
	A1-2	192.8	5.6	0.7	−0.1	A1-2	192.8	5.6	0.7	−0.1	None				
	A1-3	193.2	6.4	0.8	0.0	A1-3	193.2	6.4	0.8	0.0	None				
	A1-4	193.0	6.8	0.9	0.1	A1-4	193.0	6.8	0.9	0.1	None				
	A1-5	194.0	6.1	0.8	0.0	A1-5	194.0	6.1	0.8	0.0	None				
Avg.		193.3	6.0	0.8	0.0		193.3	6.0	0.8	0.0	None				
3 d	A3-1	191.0	27.7	3.5	0.1	W3-1	192	33.4	4.3	−0.1	None				
	A3-2	191.0	27.3	3.5	0.1	W3-2	191.5	32.8	4.2	−0.2	None				
	A3-3	190.5	27.4	3.5	0.1	W3-3	193	40.6	5.2	0.8	None				
	A3-4	191.0	28.1	3.6	0.2	W3-4	193	30.4	3.9	−0.5	None				
	A3-5	186.5	23.4	3.0	−0.4	W3-5	192.5	33.5	4.3	−0.1	None				
Avg.		190.0	26.8	3.4	0.0		192.4	34.1	4.3	0.0	None				
7 d	A7-1	190.0	56.3	7.2	−0.3	W7-1	195	66.1	8.4	−0.9	C7-1	207	64.1	8.4	0.4
	A7-2	192.0	60.4	7.7	0.2	W7-2	193	75.5	9.6	0.3	C7-2	204	64.2	8.4	0.4
	A7-3	188.0	59.9	7.6	0.2	W7-3	191	68.3	8.7	−0.6	C7-3	206	58.3	7.6	−0.4
	A7-4	194.0	60.9	7.8	0.3	W7-4	192	71.9	9.2	−0.1	C7-4	206	59.2	7.8	−0.3
	A7-5	192.0	55.6	7.1	−0.4	W7-5	193	82.7	10.5	1.2	C7-5	207	59.9	7.8	−0.2
Avg.		191.2	58.6	7.5	0.0		192.8	72.9	9.3	0.0		206	61.1	8.0	0.0
14 d	A14-1	193.5	84.1	10.7	0.3	W14-1	191.5	92.5	11.8	−1.0	C14-1	212	86.3	11.3	0.2
	A14-2	190.5	84.8	10.8	0.4	W14-2	194	111.2	14.2	1.3	C14-2	209.5	82.3	10.8	−0.3
	A14-3	194.5	82.8	10.5	0.2	W14-3	191.5	99.5	12.7	−0.2	C14-3	207.5	77.5	10.1	−0.9
	A14-4	192.5	77.4	9.9	−0.5	W14-4	191	98.1	12.5	−0.3	C14-4	211	90.4	11.8	0.7
	A14-5	195.5	78.3	10.0	−0.4	W14-5	194	102.1	13.0	0.2	C14-5	208.5	87.0	11.4	0.3

Table 5. *Cont.*

Days	Field-Cured Cylinders					Standard-Cured Cylinders					Core Samples				
	No.	L (mm)	Peak Load (kN)	f_c (MPa)	SD	No.	L (mm)	Peak Load (kN)	f_c (MPa)	SD	No.	L (mm)	Peak Load (kN)	$f_{c\text{-}eq}$ (MPa)	SD
Avg.		193.3	81.5	10.4	0.0		192.4	100.7	12.8	0.0		209.7	84.7	11.1	0.0
28 d	A28-1	187.0	82.7	10.5	−1.0	W28-1	186	144.7	18.4	−0.7	C28-1	204.5	102.5	13.4	−1.7
	A28-2	184.0	104.5	13.3	1.8	W28-2	188.5	159.3	20.3	1.2	C28-2	204.5	121.1	15.9	0.7
	A28-3	188.5	89.6	11.4	−0.1	W28-3	192	143.9	18.3	−0.8	C28-3	204	116.1	15.2	0.1
	A28-4	187.0	81.2	10.3	−1.2	W28-4	188	139.6	17.8	−1.3	C28-4	206.5	119.8	15.7	0.6
	A28-5	188.0	93.9	12.0	0.4	W28-5	190.5	162.0	20.6	1.5	C28-5	208.5	117.8	15.4	0.3
Avg.		186.9	90.4	11.5	0.0		189	149.9	19.1	0.0		205.6	115.5	15.1	0.0
91 d	A91-1	188.5	86.0	11.0	−0.4	W91-1	191.5	233.8	29.8	2.4	C91-1	204.0	150.6	19.7	0.6
	A91-2	189.5	97.0	12.4	1.0	W91-2	192.5	202.7	25.8	−1.6	C91-2	206.5	154.0	20.2	1.0
	A91-3	190.5	70.0	8.9	−2.4	W91-3	186	184.1	23.5	−4.0	C91-3	205.0	146.0	19.1	0.0
	A91-4	190.0	95.5	12.2	0.9	W91-4	189.5	215.6	27.5	0.1	C91-4	212.0	146.6	19.2	0.1
	A91-5	183.0	95.4	12.2	0.8	W91-5	190	239.4	30.5	3.1	C91-5	209.5	133.1	17.4	−1.7
Avg.		188.3	88.8	11.3	0.0		189.9	215.1	27.4	0.0		207.4	146.1	19.1	0.0

* Diameters of the cylinders were 100 mm for in-suit curing and standard curing, and 99.5 mm for the core. SD is the standard deviation.

On day 1, the measured compressive strengths (f_c) of both the standard- and field-cured cylinders were 0.8 MPa. On day 3, the f_c for standard-cured and field-cured cylinders were 4.3 MPa and 3.4 MPa, respectively, with the f_c of field-cured cylinders being approximately 30% lower than that of standard-cured cylinders (Table 5 and Figure 5).

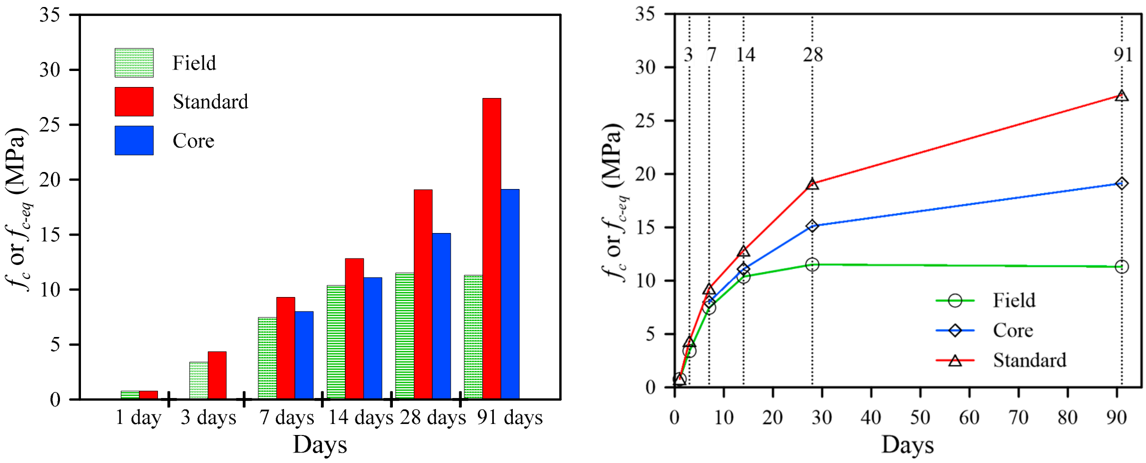

(**a**) Strengths (**b**) Development

Figure 5. Compressive strengths of concrete.

On day 7, the f_c or $f_{c\text{-}eq}$ values of the standard-cured cylinders, field-cured cylinders, and core samples were 9.3, 7.5, and 8.0 MPa, respectively. Compared with the f_c values of the standard-cured cylinders, the f_c or $f_{c\text{-}eq}$ values for the field-cured cylinders and core samples were approximately 20% and 14% lower, respectively. On day 28, the f_c or $f_{c\text{-}eq}$ values of the standard-cured cylinders, field-cured cylinders, and core samples were 19.1, 11.5, and 15.1 MPa, respectively. Compared with the f_c values of the standard-cured cylinders, the f_c or $f_{c\text{-}eq}$ values for the field-cured cylinders and core samples were approximately 40% and 20% lower, respectively. On day 91, the f_c and $f_{c\text{-}eq}$ values for the standard-cured cylinders, field-cured cylinders, and core samples were 27, 11.3, and 19.1 MPa, respectively. Compared with the f_c value of the standard-cured cylinders, the f_c or $f_{c\text{-}eq}$ values for the field-cured cylinders and core samples were approximately 59% and 30% lower, respectively. Although none of the three curing methods reached the design compressive strength (f'_c) at 28 days, the 91-day f_c for the standard-cured cylinders exceeded 24 MPa. It was reported that high levels of supplementary cementitious materials (SCMs) affect the development of concrete strength [33], and it is assumed that SCMSs delayed the development of concrete strength in this study. In contrast, the field-cured cylinders and core samples reached only 47% and 80% of their target strengths on day 91, respectively. The 28-day and 91-day f_c values for the field-cured cylinder were almost the same, indicating that the compressive strength did not improve significantly. Overall, the unmanaged and cool curing environment affected the concrete strength development. It was assumed that high levels of SCMs delay the development of concrete strength, and unmanaged and cool curing conditions interfered with long-term development. Consequently, it is assumed that the compressive strength at 91 days of the field-cured cylinders and core samples was lower than that of the standard-cured cylinders.

3.4. Discussion on the Relationship between Maturity and Compressive Strength

The maturity indices and compressive strengths for various curing methods and hydration heat measurements within 7 days are summarized in Table 6, and Figure 6 depicts the trend of relation between maturity and development of compressive strength. On day 3, the M value for field curing was 5% lower than that for standard curing; however, the f_c value was 21% lower. On day 7, the M value for field curing was 7% lower than that for standard curing; however, the f_c value was 19% lower. The M values for wire/wireless in the RC slab were 6% lower than those for standard curing; however, the $f_{c\text{-}eq}$ value was 14% lower. The difference in M values between standard and wire field, wire slab, and wireless slab was within 7%; however, the difference in compressive strength was greater, ranging from 14% to 19%, which was larger than the difference in M values.

Table 6. Comparison of concrete strengths and maturity at early ages.

Days	Index	Standard Curing	Field Curing	RC Slab	
			Wire	Wire	Wireless
1 (24 h)	Maturity (°C·h) [Ratio]	711 [1.00]	711 [1.00]	723 [1.02]	711 [1.00]
	f_c (MPa) [Ratio]	0.8 [1.00]	0.8 [1.00]	-	-
3 (72 h)	Maturity (°C·h) [Ratio]	2151 [1.00]	2041 [0.95]	2073 [0.96]	2103 [0.98]
	f_c (MPa) [Ratio]	4.3 [1.00]	3.4 [0.79]		
7 (168 h)	Maturity (°C·h) [Ratio]	5031 [1.00]	4665 [0.93]	4741 [0.94]	4723 [0.94]
	f_c or $f_{c\text{-}eq}$ (MPa) [Ratio]	9.3 [1.00]	7.5 [0.81]	8.0 [0.86]	8.0 [0.86]

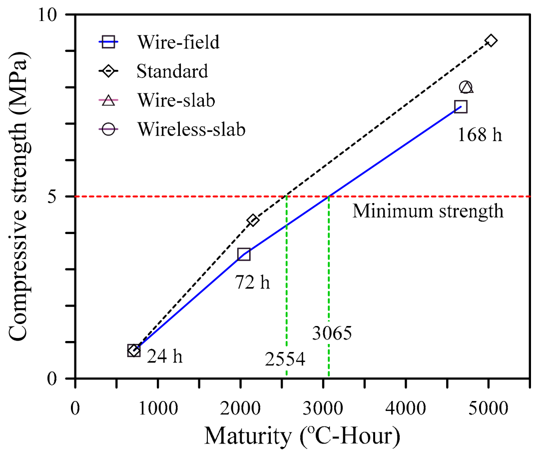

Figure 6. Relation of compressive strength and maturity.

In this experiment, even without watering and protection, the compressive strength of the field-cured cylinders was 3.4 MPa on day 3 and 7.5 MPa on day 7. Linear interpolation was used to determine the point at which the strength reached 5 MPa, which was approximately 106.5 h, or 5 days. This corroborates the criteria in KCS 14 20 10 [19] for removing the formwork panels of foundations, sides of beams, columns, and walls without evaluating the compressive strength.

4. Conclusions

This study evaluated the performance of commercial IoT-based wireless thermocouple sensors and conventional wire thermocouple sensors, including in cool environments that lacked water and protection. Furthermore, it collated data related to the development of concrete strength under unmanaged and cool environments. The early age maturity and concrete compressive strength within the first 7 days were also compared.

In the RC slab, wire thermocouple sensors and IoT-based wireless thermocouple sensors were installed at five identical locations to measure the hydration heat. The average difference in the hydration heat values measured by the two types of sensors over 7 days (168 h) was within 1%, indicating almost identical results. In the same environment as the RC slab, five field-cured cylinders were manufactured, and their hydration heat was measured using wire thermocouple sensors, with the 168-h maturity values showing a difference within 2% compared with those measured by wire thermocouple sensors in the RC slab. This suggests that IoT-based wireless thermocouple sensors can replace wire thermocouple sensors for evaluating early age compressive strength. Moreover, it was deemed acceptable to use the values from field-cured cylinders instead of directly installing thermocouple sensors in the RC slab.

Omitting watering and protection in cool environments significantly affects the development of concrete compressive strength. Compared with standard-cured cylinders, the compressive strengths of field-cured cylinders and core samples were 19% and 14% lower on day 7, 40% and 20% lower on day 28, and 59% and 30% lower on day 91, respectively. This study found that in cool environments, the absence of watering and protection significantly influences the development of concrete strength. In particular, field curing was particularly affected, which made indirect evaluation of the structural compressive strength challenging. When curing concrete with high levels of SCMs, curing management is considered necessary to develop long-term strength.

This study set an unmanaged and cool environment as the curing condition. In order to determine the feasibility of IoT-based wireless sensors, follow-up research is needed on various harsh curing conditions such as frozen, cool, and humid, etc. Conducting experiments considering various concrete mixtures and developing models according to curing conditions is also necessary.

Author Contributions: Conceptualization, D.J. and S.K.; methodology, J.-H.M.; software, J.-Y.K. and S.K.; formal analysis, J.-Y.K. and S.K.; investigation, D.J. and J.-H.M.; resources, S.K. and J.-H.M.; data curation, S.K.; writing—original draft preparation, S.K.; writing—review and editing, D.J.; visualization, J.-Y.K.; supervision, S.K.; project administration, S.K. All authors have read and agreed to the published version of the manuscript.

Funding: This work was supported by National Research Foundation of Korea (NRF) Grant (NRF-2021R1I1A2048618 and 2022R1A4A5028239).

Data Availability Statement: The raw data supporting the conclusions of this article will be made available by the authors on request.

Conflicts of Interest: The authors declare no conflict of interest.

References

1. Nilimaa, J.; Gamil, Y.; Zhaka, V. Formwork Engineering for Sustainable Concrete Construction. *CivilEng* **2023**, *4*, 1098–1120. [CrossRef]
2. Sharma, S.; Dangi, S.K.; Bairwa, S.K.; Sen, S. Comparative study on sensitivity of acceleration and strain responses for bridge health monitoring. *J. Struct. Integr. Maint.* **2022**, *7*, 238–251. [CrossRef]
3. Saidin, S.S.; Jamadin, A.; Kudus, S.A.; Amin, N.M.; Anuar, M.A. An Overview: The Application of Vibration-Based Techniques in Bridge Structural Health Monitoring. *Int. J. Concr. Struct. Mater.* **2023**, *17*, 251–267. [CrossRef]
4. Castillo, D.; Hedjazi, S.; Kabir, E. Study on Early-Age Elastic Modulus of FRC Using Electrical Resistivity and Resonance Frequency. *Int. J. Concr. Struct. Mater.* **2023**, *17*, 1–13. [CrossRef]
5. Kumar, S.; Rai, B. Synergetic Effect of Fly Ash and Silica Fume on the Performance of High Volume Fly Ash Self-Compacting Concrete. *J. Struct. Integr. Maint.* **2022**, *7*, 61–74. [CrossRef]
6. Yoon, I.-S.; Chang, C.; Nam, J.-W. Effect of Carbonation on Chloride Transportation Parameters in Cementitious Materials. *J. Struct. Integr. Maint.* **2022**, *7*, 161–167. [CrossRef]
7. *ACI 228.IR-03*; ACI Committee 228, In-Place Methods to Estimate Concrete Strength. America Concrete Institute: Farmington Hills, MI, USA, 2003.
8. *ACI 228.1R-19*; ACI Committee 228, Report on Methods for Estimating In-Place Concrete Strength. America Concrete Institute: Farmington Hills, MI, USA, 2019.
9. Tekle, B.H.; Al-Deen, S.; Anwar-Us-Saadat, M.; Willans, N.; Zhang, Y.; Lee, C.K. Use of Maturity Method to Estimate Early Age Compressive Strength of Slab in Cold Weather. *Struct. Concr.* **2022**, *23*, 1176–1190. [CrossRef]

10. *ASTM C42/C42M-20*; Standard Test Method for Obtaining and Testing Drilled Cores and Sawed Beams of Concrete. ASTM International: West Conshohocken, PA, USA, 2022.
11. *ACI 214.4R-03*; ACI Committee 214, Guide for Obtaining Cores and Interpreting Compressive Strength Results. America Concrete Institute: Farmington Hills, MI, USA, 2003.
12. *ASTM C805/C805M-18*; Standard Test Method for Rebound Number of Hardened Concrete. ASTM International: West Conshohocken, PA, USA, 2019.
13. *ASTM C803/C803M-18*; Standard Test Method for Penetration Resistance of Hardened Concrete. ASTM International: West Conshohocken, PA, USA, 2019.
14. *ASTM C900-19*; Standard Test Method for Pullout Strength of Hardened Concrete. ASTM International: West Conshohocken, PA, USA, 2020.
15. *ASTM C1583/C1583M-20*; Standard Test Method for Tensile Strength of Concrete Surfaces and the Bond Strength or Tensile Strength of Concrete Repair and Overlay Materials by Direct Tension. ASTM International: West Conshohocken, PA, USA, 2020.
16. *ASTM C597-22*; Standard Test Method for Ultrasonic Pulse Velocity through Concrete. ASTM International: West Conshohocken, PA, USA, 2023.
17. *ASTM C1074-19el*; Standard Practice for Estimating Concrete Strength by the Maturity Method. ASTM International: West Conshohocken, PA, USA, 2019.
18. *ASTM C873/C873M-15*; Standard Test Method for Compressive Strength of Concrete Cylinders Cast in Place in Cylindrical Molds. ASTM International: West Conshohocken, PA, USA, 2016.
19. *KCS 14 20 10*; General Concrete, Korea Construction Standard Center. Korea Concrete Institute: Sejong, Republic of Korea, 2022. (In Korean)
20. Yikici, T.A.; Chen, H.-L. Use of maturity method to estimate compressive strength of mass concrete. *Constr. Build. Mater.* **2015**, *95*, 802–812. [CrossRef]
21. Ma, Q.; Xiao, J.; Ding, T.; Duan, Z.; Song, M.; Cao, X. The prediction of compressive strength for recycled coarse aggregate concrete in cold region. *Case Stud. Constr. Mater.* **2023**, *19*, e02546. [CrossRef]
22. Boubekeur, T.; Ezziane, K.; Kadri, E.-H. Estimation of mortars compressive strength at different curing temperature by the maturity method. *Constr. Build. Mater.* **2014**, *71*, 299–307. [CrossRef]
23. Kampli, G.; Chickerur, S.; Chitawadagi, M.V. Real-time in-situ strength monitoring of concrete using maturity method of strength prediction via IoT. *Mater. Today Proc.* **2023**, *88*, 110–118. [CrossRef]
24. Miller, D.; Ho, N.-M.; Talebian, N.; Javanbakht, Z. Real-time monitoring of early-age compressive strength of concrete using an IoT-enabled monitoring system: An investigative study. *Innov. Infrastruct. Solut.* **2023**, *8*, 75. [CrossRef]
25. Mun, D.-H.; Jang, H.-O.; Lee, H.-S. An Experimental Study on the Prediction of Concrete Compressive Strength by the Maturity Method Using Embedded Wireless Temperature and Humidity Sensor. In *Proceedings of the Korean Institute of Building Construction Conference*; Korea Institute of Science and Technology Information: Daejeon, Republic of Korea, 2018; Volume 18, pp. 94–95. (In Korean)
26. Lee, Y.J.; Hyun, S.Y.; Kim, T.W.; Lee, S.W.; Han, M.C.; Han, C.G. Strength monitoring of the wall concrete using insulation formwork and unreinforced formwork using maturity based wireless sensor network. In *Proceedings of the Korea Concrete Institute*; Korea Institute of Science and Technology Information: Daejeon, Republic of Korea, 2018; Volume 1, pp. 325–326. (In Korean)
27. *ASTM C31/C31M-22*; Standard Practice for Making and Curing Concrete Test Specimens in the Field. ASTM International: West Conshohocken, PA, USA, 2022.
28. *KS L 5210*; Portland Blast-Furnace Slag Cement. Korean Agency for Technology and Standards: Eumseong, Republic of Korea, 2023. (In Korean)
29. *KS L 5405*; Fly Ash. Korean Agency for Technology and Standards: Eumseong, Republic of Korea, 2018. (In Korean)
30. Saul, A.G.A. Principles underlying the steam curing of concrete at atmospheric pressure. *Mag. Concr. Res.* **1951**, *2*, 127–140. [CrossRef]
31. Jo, S.D.; Kwon, S.H.; Kim, C.Y.; Park, Y.S. Effect of Damage Caused by Extracting Cores on Compressive Strength of Concrete. *J. Korea Concr. Inst.* **2019**, *31*, 397–405. (In Korean) [CrossRef]
32. Oh, H.; Oh, K.-C. An Empirical Approach for Improving the Estimation of the Concrete Compressive Strength Considered the Effect of Age and Drilled Core Sample. *J. Korea Inst. Struct. Maint. Insp.* **2015**, *19*, 103–111. (In Korean)
33. Nilimaa, J. Smart Materials and technologies for sustainable concrete construction. *Dev. Built Environ.* **2023**, *15*, e100177. [CrossRef]